Dynamic wind power simulation

Dougal McQueen, Alan Wood, and Allan Miller
Electric Power Engineering Centre, University of Canterbury, New Zealand.
Email: dougal.mcqueen@pg.canterbury.ac.nz

EEA Conference & Exhibition 2016, 22 - 24 June, Wellington

Abstract

Wind energy is one of the least cost methods of electricity generation, produces no carbon emissions, and is highly scaleable. However, the intermittency of wind and the passive reaction of wind turbines means spinning and scheduled reserves are required to ensure grid security. It is important for power system planning that temporally and spatially accurate models of wind power are formulated. While the simulation of wind speed time-series is well defined the transformation from wind speed to wind power time-series is less so. Wind power plants comprise arrays of wind turbines and the individual wind turbine power time-series are not independent; thus a temporally consistent model for the spatial correlation of the wind resource is required. The spatial correlation of the wind resource can be separated into steady state and dynamic factors. Here the steady state factors are modelled using the Measure Correlate Predict algorithm and the dynamic factors modelled using the Sandia method. However, the Sandia method does not accommodate the heteroskedasticity inherent in turbulence thus a method using Wavelet Multi-resolution Analysis is developed and validated against measurements made at a wind power plant in New Zealand. The Sandia and Wavelet Multi-resolution Analysis models are numerically complex and not suited to simulations involving large number of wind power plants hence the equivalence to a first order low pass filter is demonstrated.

1 Introduction

Time-series models for wind power are necessary to enable the effects of greater penetration of wind energy into electricity networks to be determined. It is possible to use historic measurements, or meteorological model outputs, to develop coherent sets of wind speed time-series (WSTS) that are representative of envisaged wind power plants (WPP) [1]. The WSTS must be transformed to the corresponding wind power time-series. For the wind power time-series to be truly representative of the WPP the transform must be accurate for both the steady-state and dynamic characteristics.

The transformation from wind speed to power by an individual wind turbine is well characterised by the wind turbine power curve (often calibrated using IEC-61400-12 [2]). However, a WPP comprises a group of spatially distributed wind turbines, and the WPP power curve is more enigmatic. The wind turbines are spaced apart so they do not suffer undue fatigue due to turbulence induced in turbine wakes, and capture the maximum amount of energy. WPP topography is not always uniform, thus each turbine will experience different wind speeds. This spread of wind speeds can be modelled as a steady state function by smoothing the wind turbine power curve [3].

Further, the winds incident on wind turbines are not independent; turbines in close proximity fetch similar wind hence produce more strongly correlated power than turbines farther apart. The correlation structure is the result of turbulence and the reaction of the wind turbines to turbulence also defines the dynamic character of the power.

Data from the Mt Stuart WPP are used to develop and apply models for simulating wind power. Measurements made at the meteorological mast are used to provide a reference wind speed and direction time-series. This WSTS is transformed to be representative of the wind incident on individual turbines using the Measure-Correlate-Predict (MCP) methodology, accounting for steady state characteristics. The MCP model is coupled to the Sandia method, to account for turbulence. However, the Sandia method does not allow the heteroskedasticity inherent in turbulence to be characterised, hence a Wavelet Multi-resolution Analysis (WMA) approach is developed. The Sandia and WMA methods are numerically complex and are not appropriate for simulating the power from fleets of WPPs hence the equivalence to a first order low pass filter (LPF) is demonstrated.

The simulated power time-series are modified by a Markov chain model, derived from the operational data, to account for operational efficiency (as applied by Sulaeman [4]). The resultant power time-series are compared with measurements made at the Mt Stuart WPP.

2 Mt Stuart Wind Power Plant

The Mt Stuart WPP comprises nine 850 kW Gamesa G52 wind turbines (total 7.65 MW) with a hub height of 45 m, stretching north to south in a single line across the top of Mt Stuart. The wind turbine power curve for the Gamesa G52 turbine has been obtained from sales documentation [5]. Mt Stuart is in South Otago, New Zealand, and is elevated above the rolling hill country, well exposed to the prevailing westerly winds. Each wind turbine has a cup anemometer mounted on the rear of the nacelle. The WPP also has a 30 m meteorological mast, sited between turbines, near the middle of the WPP. Power, wind speed, and nacelle orientation for each turbine, as well as total WPP power, and meteorological mast wind speed and direction data have been extracted from the SCADA, at a resolution of 1 min, for a period of one year.

The WSTS derived from the nacelle anemometers have a high pass filter applied to assist in turbine fault diagnostics. Further the nacelle anemometers are located behind the turbine rotor and are affected by the rotor wake and the nacelle bulk. It is necessary to scale the nacelle WSTS such that they are representative of the free stream wind speed. Kolmogorov's theory for the spectral energy density, as presented in Equation 1, is used as a target to scale the nacelle WSTS [6]. The effect of the scaling is illustrated in Figure 1.

$$E(k) = C\epsilon^{\frac{2}{3}}(\frac{f}{\bar{u}})^{\frac{-5}{3}} \tag{1}$$

Where E is the energy density, C is a universal constant, ϵ is the eddy viscosity, f is the frequency, and $\bar{u}$ is the mean wind speed.

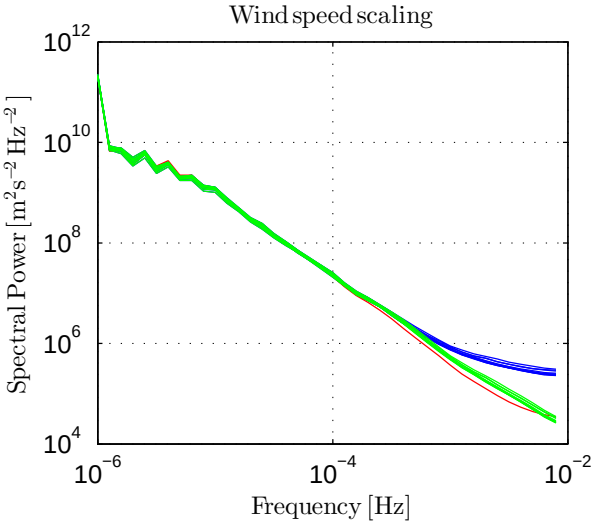

Figure 1: Kolmogorov scaling: nacelle wind speed power spectra shown by blue lines, scaled power spectra shown by green lines, and power spectra from meteorological mast shown by red line.

3 MCP

The relative wind speed between two points in close proximity for a given wind direction is well approximated by a linear regression. This linear regression reflects differences in exposure and can be reconciled as a steady state transformation. The MCP methodology defined by Derrick makes use of this property [7]. In the application here the WSTS from the meteorological mast and nacelle anemometers are averaged such that they are approximately concomitant (a temporal resolution of 64 min). The WSTS at the meteorological mast is binned into twelve 30° sectors (with periods when the wind speed is less than $3ms^{-1}$ excluded). For each turbine, in each direction sector, a single parameter linear regression is found using least squares forced through the origin. The resulting slope is termed the "speed up". The speed ups are then applied to the WSTS measured at the meteorological mast to obtain WSTS for each turbine as shown in Equation 2.

$$u_N(t) = S_{(\theta,N)} \cdot u_M(t) \tag{2}$$

Where u is the wind speed, N is the turbine index, t is time, θ is the wind direction sector, S is the speed up, and M denotes the meteorological mast.

4 Sandia method

While the ratio of wind speeds between two points has a tendency toward the speed ups defined using the MCP method; the speed ups change dynamically as a result of the propagation of eddies across the landscape. The Sandia method models the coherence between points and is used to impute the WSTS [8]. The coherence between points is modelled as a function of separation distance, frequency, and mean wind speed, as defined by Davenport, and presented in Equation 3 [9].

$$\Gamma(f, r, \bar{u}) = e^{-d\frac{r}{\bar{u}}f} \tag{3}$$

Where Γ is the coherence, f is frequency, r is separation distance, d is the decay constant (a value of 7 is applied; representative of low coherence, or complex terrain, as suggested by Nanahara et al. [10]), and $\bar{u}$ is the mean wind speed.

A WPP power time-series can be simulated using MCP and the Sandia method by:

1. For each turbine white noise time-series are generated. Fourier transforms are applied to find the power spectra and these coloured to Kolmogorov's spectra (as defined in Equation 1).
2. Coherence matrices are defined for each frequency using Davenport's relationship, and the distance between each turbine pair. The set of complex power spectra are multiplied by the Cholesky decompositions of the coherence matrices to obtain a set of correlated power spectra.
3. The low frequency components of the power spectra are substituted with power spectra obtained from the MCP scaled WSTS (equivalent to the method described by Rose and Apt [11]).
4. Inverse Fourier transforms are applied to the resultant power spectra to find time-series representative of the wind speed incident at each wind turbine.
5. The WSTS are transformed to power by applying the wind turbine power curve, and the WPP power found as the aggregate of these.

The MCP / Sandia method characterises the spatial integration over a WPP. However, the inertia and spatial integration of a wind turbine is not accounted for. The averaging of a wind turbine should be evident as differences in power spectral densities (PSD) of the measured wind turbine power and that simulated. However, the use of the Kolmogorov spectrum as a target for filtering nacelle wind speeds removes veracity of the simulated spectra and results show no substantial difference between simulated and measured spectra. While it is intuitive that the wind turbine PSD should differ from that measured using a cup anemometer it should be noted that wind turbines are mechanically complex, experiencing phenomena such as blade / tower interactions, thus are not representative of free stream measurements.

5 WMA

Turbulence is the result of the progression of eddies or vortices of varying sizes past a point, and is advected with the bulk movement of air. The magnitude of the turbulence

is proportional to the wind speed, as such a WSTS is heteroskedastic.

The physical size of the eddies determines both the spatial extent and the temporal duration of their influence. Thus it is intuitive to decompose a time-series into a form whereby the influence of small scale eddies, that have local influence, are isolated from the larger eddies. Davenport's relationship is reliant upon the Fourier expansion and retains no information as to when in time an eddy processes hence assumes homoskedasticity.

Wavelet decomposition allows a time-series to be represented in the time-frequency plane using a dyadic structure. A wavelet is a compact oscillatory function that is square integrable as presented in Equation 4. The decomposition, at each scale, is achieved by deconvolving the time-series by the wavelet, resulting in a wavelet coefficient series and a residual time-series, as presented in Equation 5. The wavelet series and residual time-series have a temporal resolution half that of the initial time-series. The residual time-series can be recursively decomposed by dilating the wavelet (by an order of two to ensure a dyadic structure), and deconvolving to obtain further wavelet coefficient series and residual time-series. The wavelet decomposition is achieved using the tools in the WaveLab toolbox for Matlab [12].

$$\{\psi_{j,\tau}(t) = \frac{1}{\sqrt{2^j}}\psi\left(\frac{t-2^j\tau}{2^j}\right)\}_{(j,\tau)inZ^2} \tag{4}$$

Where ψ is the mother wavelet, j is the scale, and τ is the translation.

$$\langle u(\tau,2^j),\Psi(j,\tau)\rangle = \int_{-\infty}^{\infty} u(t)\frac{1}{\sqrt{j}}\psi^*\left(\frac{t-\tau}{j}\right)dt \tag{5}$$

Where Ψ is the wavelet coefficient series, t is time, and * denotes the complex conjugate.

The wavelet decomposition results in a number of wavelet series and a residual time-series increasing the dimensionality of the set of time-series; the set of wavelet series having auto-correlations (see Equation 6), correlations between the wavelet series resulting from different time-series at the same scale (see Equation 7), and cross-correlation between wavelet series of adjacent scales (see Equation 8). To make simulation tractable it is necessary to reduce the dimensionality through careful selection of the wavelet. A variety of wavelets have been tested and the Beylkin wavelet is found to minimizes the cross-correlation.

$$\begin{aligned} R(\Psi_n(j,\tau),\Psi_n(j,\tau+\delta)) = \sum_{\tau=1}^{T}\{&(\Psi_n(j,\tau)-\overline{\Psi_n(j,\tau)}) \\ &(\Psi_n(j,\tau+\delta)-\overline{\Psi_n(j,\tau+\delta)})\} \end{aligned} \tag{6}$$

Where R is the Pearson's correlation coefficient, n is a measurement, and $\Psi_n(j,\tau)$ is the temporal average of the wavelet coefficients.

$$\begin{aligned} R(\Psi_n(j),\Psi_m(j)) = \sum_{\tau=1}^{T}\{&(\Psi_n(j,\tau)-\overline{\Psi_n(j,\tau)}) \\ &(\Psi_m(j,\tau)-\overline{\Psi_m(j,\tau)})\} \end{aligned} \tag{7}$$

Where m is a second measurement.

$$R(\Psi_n(j), \Psi_n(j+1)) = \sum_{\delta=[-\frac{1}{4},\frac{1}{4}]} \sum_{\tau=1}^{T} \{(\Psi_n(j,\tau) - \overline{\Psi_n(j,\tau)}) \\ (\Psi_n(j+1,\tau+\delta) - \overline{\Psi_n(j+1,\tau+\delta)})\} \tag{8}$$

The purpose of the wavelet decomposition is to separate turbulent eddies of different spatial and temporal scales. It is expected that larger eddies will affect points that have greater spatial separation. In Figure 2 each dot represents the correlation between wavelet series. For example it is seen that for turbines separated by greater than 200 m the correlation at a scale of 2 minutes is near zero, and the correlation well described using a log-linear function for distances less than 200 m.

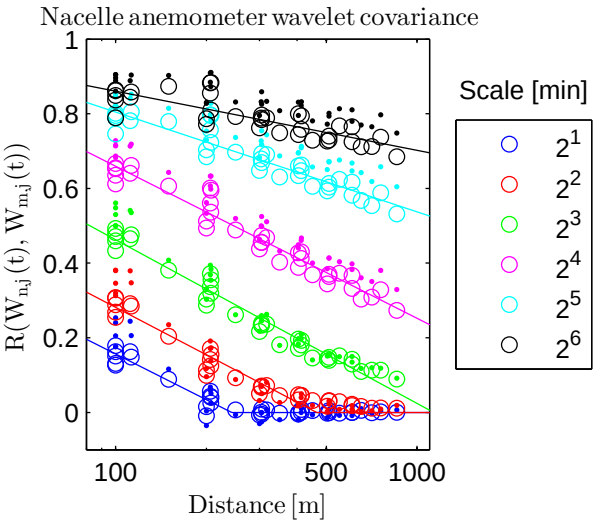

Figure 2: Wavelet covariance

The wavelet series can be modelled as Auto-Regressive processes; however to do so they must be transformed to stationary Gaussian processes. It is found that the magnitude of the wavelet series is related to the magnitude of the residual time-series thus a Taylor transform is applied as shown in Equation 9. The Taylor co-efficients are found using an optimisation search such that the correlation between the transformed wavelet series and the residual time-series equals zero. The resulting Taylor transformed wavelet series are observed to be non-Gaussian, thus a Johnson transform is applied (as shown in Equation 10), the fitting and application of which is achieved through the use of the Johnson Curve Toolbox for Matlab [13]. These transformations may affect the correlation structures of the wavelet-series, hence the distance relationships in Figure 2 are reaffirmed with circles representing the correlations for the Taylor-Johnson transformed wavelet series ($\Psi_n^{(TJ)}$).

$$\Psi_n^{(T)}(j,\tau) = \frac{\Psi(j,\tau)}{\bar{u}(t)^a} \tag{9}$$

Where a is the Taylor exponent, and T represents the Taylor transformed variable.

$$\Psi n^{(TJ)}(j,\tau) = \gamma + \eta \, sinh^{-1}\left(\frac{\Psi_n^{(T)}(j,\tau) - \epsilon}{\lambda}\right) \tag{10}$$

Where J represents the Johnson transformed variable, γ and η are shape parameters, ϵ is the location parameter, and λ is the scale parameter.

The Taylor-Johnson transformed wavelet series from the nacelle anemometers comprise sets of Gaussian processes and these approximated as an AR process. The Box-Jenkins method using correlograms and partial-correlograms identifies the $\Psi_n^{(TJ)}(j)$ series as an over-differenced AR processes with a model order of 1 [14]. A Correlated Innovation Matrix (CIM) approach is applied, as described in Equation 11, to simulate the wavelet series.

$$\begin{aligned}\Psi_n^{(TJ)}(j,\tau) =& A_\alpha(j)\cdot\Psi_n^{(TJ)}(j,\tau-\alpha)+ \\ & A_{\alpha-1}(j)\cdot\Psi_n^{(TJ)}(j,\tau-(\alpha-1))+\cdots+ \\ & A_1(j)\cdot\Psi_n^{(TJ)}(j,\tau-1)+\zeta\cdot e_t\end{aligned} \tag{11}$$

Where A_α is the AR coefficient of order α, ζ is the CIM loci, and e is the innovation matix.

Wind power time-series for a WPP can be simulated using the following procedure:

1. The MCP scaled WSTS, as developed in Section is scaled by a factor of $\sqrt{2^6}$ and placed into the residual time-series portion of the wavelet structure.
2. For each scale 2^1 through 2^6 minutes wavelet series are simulated. These series are generated using the CIM approach, the CIM loci (ζ) are defined using the Cholesky decomposition of the matrix formed using the turbine separation distances and log-linear relationships (as presented in Figure 2). The CIM series are inverse Johnson and inverse Taylor transformed and the resultant series appropriated into the wavelet structure. The parameters for the Johnson and Taylor transformations are derived for each scale from the mean values found for the Mt Stuart data.
3. The inverse wavelet transformation is applied to the simulated wavelet structures to find wind speed time series representative of each wind turbine.
4. The WSTS are transformed to power using the wind turbine power curve, and the WPP power time-series calculated as the aggregate of the wind turbine power time-series.

Model parameters are presented in Table 1.

Table 1: WMA model parameters

Scale [min]	Taylor exp.	Johnson coeffs				AR coeffs
	a	γ	η	ϵ	λ	A_1
2	0.67	-0.03	1.4	0	0.07	-0.27
4	0.61	0.01	1.4	0	0.16	-0.24
8	0.54	0.01	1.5	0	0.34	-0.24
16	0.48	0.02	1.5	0	0.66	-0.24
32	0.46	0.02	1.6	0	1.22	-0.23
64	0.41	-0.03	1.7	0	2.6	-0.23

6 Low Pass Filter

The spatial integration of wind turbines can be modelled using a first order low pass filter as described in Equation 12 and proposed by Madsen in 1984 [15]. The low pass filter constant for the Mt Stuart WPP is found by minimising the root-mean-square difference

in measured and simulated power spectral densities of WPP power time-series and for Mt Stuart equals 34.

$$u_{\omega'} = F'\{\frac{F(u)}{1 - M\omega}\} \tag{12}$$

Where ω is frequency, F denotes the Fourier transform, F' the inverse Fourier transform, and M is the low pass filter constant.

The wind power time-series is found by applying the low pass filter to the WSTS from the meteorological mast, and subsequently applying the WPP power curve. The WPP power curve is found by applying a Gaussian distribution of speed ups to the wind turbine power curve as shown in Equation 13. The mean and standard deviation for the speed ups are taken from the frequency weighted average of all speed ups derived in Section 1.

$$P_S(u) = \int_{q=0}^{1} P(u \cdot S_{\mu_g,\sigma_g}(q)) \tag{13}$$

Where q is probability.

7 WPP Efficiency

The WPP power output is lower than the hypothetical power due to electrical losses, turbine wakes, and operational efficiency. Electrical and wake losses for the Mt Stuart WPP are small and thus omitted for the models. The operational efficiency (often referred to as the availability) describes the ratio of power produced to that which would be produced if all turbines were operating in an unrestricted manner. Turbines may be restricted due to faults or maintenance. The operational efficiency has been calculated using data from the Mt Stuart WPP; the average operational efficiency for the period being 97%. A Markov Chain (MC) model, as described by Sulaeman [4], is applied to simulate the operational efficiency. The transition matrix is constructed assuming wind turbines can only be either on or off, thus a total of 10 operational states are possible. The MC model is used to generate operational efficiency time-series and these used to adjust the simulated WPP power time series.

Note that for a WPP with a small number of wind turbines the relative step change in power output due to turbines being shut down or started is large, hence the accuracy of the MC model is important for the accuracy of ramp rate prediction.

8 Results

The effect of accounting for heteroskedasticity in simulation of WSTS on the power time-series is demonstrated in Figure 3. The top graph presents the variance of wind speed, or turbulence, as a function of wind speed. The measured data show the definite relationship between turbulence and wind speed, and this is replicated by the WMA model, whereas the Sandia method has no such dependence. However, once converted to power the benefit of including heteroskedasticity is not apparent as the operational characterisitcs of the wind turbines become important.

Results are coloured according to the following legend:

- Measured = black,
- Sandia method = blue,

- WMA = green,
- LPF = red.

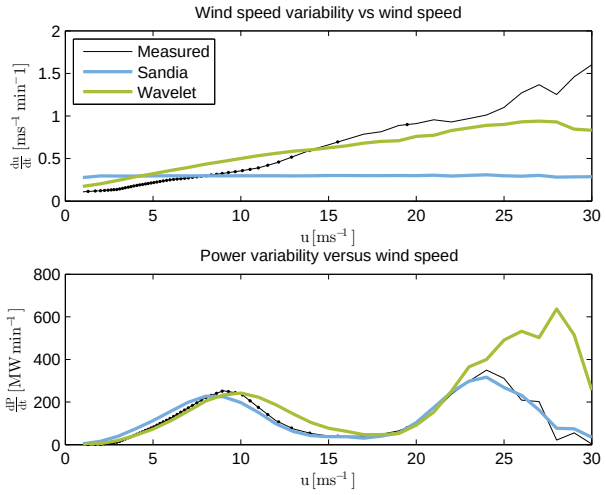

Figure 3: Effect of heteroskedasticity on simulated power

The operational characterisitcs of the turbines have not been modelled further than application of the power curve. Of particular importance is the control of turbines at high wind speeds; turbines shut down at a high wind speed limit and do not restart until the wind speed drops below a lower limit creating a high wind hysteresis loop. The turbine control system is complex and details proprietary, if the turbine control system could be explicitly modelled the value of simulating the heteroskedasticity may become apparent. Further, the integration by the rotor has not been modelled and the degree of integration depends on the wind speed.

Results for WPP power simulations are presented in Figure 4. The top graph presents probability density functions (PDF) for wind power plant time-series derived from measurements and simulations. The PDFs are all similar, to the point of replicating the spikes at integer multiples of turbine rated power.

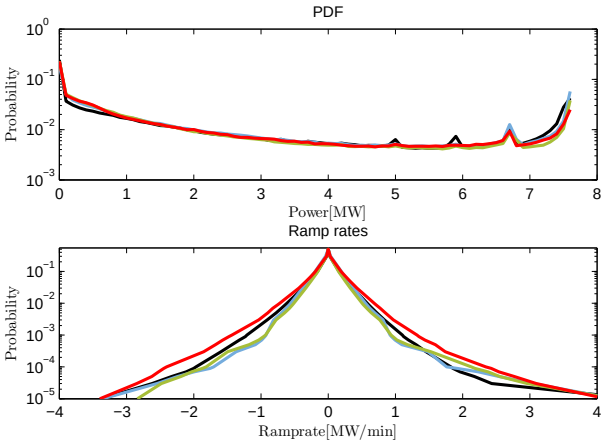

Figure 4: Probability density functions and ramp rates for Mt Stuart

The lower graph in Figure 4 presents probability distribution functions for changes in power, or ramp rates, across a 1 min interval. The replication of ramp rates is crucial

for supporting power system stability studies and reflects the dynamic response of wind turbines to turbulence. The Sandia and WMA models agree very well with measured values and there is little to differentiate the models. The power time-series derived from the low pass filter model tends to over estimate ramp rates by approximately 20%.

9 Conclusion

The simulation of wind power time-series is necessary for determining the effects of integrating WPPs into power systems. Models for wind power are derived using measured WSTS applying methods to account for the spatial diversity. Firstly, a model using the MCP algorithm and the Sandia method is constructed. However, it is noted that the Sandia method assumes homoskedasticity and it is shown that WSTS are heteroskedastic, hence a model utilising WMA is developed. These models produce WSTS incident at wind turbines and these are transformed to power using the wind turbine power curve. The aggregate of the turbine power time-series provides the WPP power time-series. As the Sandia and WMA models are numerically complex and not appropriate in simulations involving fleets of wind farms a model using a first order low pass filter and wind farm power curve is applied.

The Sandia based method is shown to accurately reproduce the wind speed to power relationship. The WMA model is found to not increase accuracy showing the importance of explicitly modelling the wind turbine control system if the dependence on heteroskedasticity is to be verified. Further, the methods presented are compromised by filtering applied to the nacelle mounted anemometers. The exact nature of the filter is unknown so pragmatic scaling is applied.

The methods developed are based on measurements made at a single WPP. Thus simulations are limited to be representative of WPPs utilising Gamesa G52 wind turbines in rolling hill country. It is posited that wind turbines will provide some smoothing of the wind due to integration over their rotor area and inertia; however, no change in PSD evident. This may not be the case for larger wind turbines. The analysis in this paper presents methods for simulating dynamic wind power, the results could be further developed using data from WPPs with different topographies and wind turbine types.

Acknowledgment

This work is part of the GREEN Grid project funded by Ministry Business Innovation and Employment, New Zealand. www.epecentre.ac.nz/greengrid Thanks to Pioneer Generation Limited for the supply of data from the Mt Stuart Wind Farm.

References

[1] N. J. Cutler, H. R. Outhred, I. F. MacGill, M. J. Kay, and J. D. Kepert, "Characterizing future large, rapid changes in aggregated wind power using numerical weather prediction spatial fields," *Wind Energy*, vol. 12, no. 6, pp. 542–555, 2009.

[2] IEC, "Wind turbines part 12-1: Power performance measurements of electricity producing wind turbines," 2005.

[3] G. McNerney and R. Richardson, "The statistical smoothing of power delivered to utilities by multiple wind turbines," *Energy Conversion, IEEE Transactions on*, vol. 7, no. 4, pp. 644–647, 1992.

[4] S. Sulaeman, M. Benidris, and J. Mitra, "A method to model the output power of wind farms in composite system reliability assessment," in *North American Power Symposium (NAPS), 2014*, 2014, pp. 1–6.

[5] Gamesa, "Gamesa g52-850 kw," 2007.

[6] R. B. Stull, *An introduction to boundary layer meteorology*, ser. Atmospheric sciences library. Kluwer Academic, 2003, c1988.

[7] A. Derrick, "Development of the measurecorrelatepredict strategy for site assessment," 1993.

[8] P. S. Veers, "Three-dimensional wind simulation," in *Eighth ASME Wind Energy Symposium, January 22, 1989 - January 25, 1989*, ser. American Society of Mechanical Engineers, Solar Energy Division (Publication) SED, vol. 7. Publ by American Soc of Mechanical Engineers (ASME), 1988, pp. 23–31.

[9] A. G. Davenport, "The spectrum of horizontal gustiness near the ground in high winds," *Quarterly Journal of the Royal Meteorological Society*, vol. 87, no. 372, pp. 194–211, 1961.

[10] T. Nanahara, M. Asari, T. Sato, K. Yamaguchi, M. Shibata, and T. Maejima, "Smoothing effects of distributed wind turbines. part 1. coherence and smoothing effects at a wind farm," *Wind Energy*, vol. 7, no. 2, pp. 61–74, 2004.

[11] S. Rose and J. Apt, "Generating wind time series as a hybrid of measured and simulated data," *Wind Energy*, vol. 15, no. 5, pp. 699–715, 2012.

[12] S. Mallat, *A Wavelet Tour of Signal Processing, Third Edition: The Sparse Way*. Academic Press, 2008.

[13] D. L. Jones, "The johnson curve toolbox for matlab: analysis of non-normal data using the johnson system of distributions," 2014.

[14] H. Ltkepohl, *New Introduction to Multiple Time Series Analysis*. Springer, 2007.

[15] W. Schlez, "Voltage fluctuations caused by groups of wind turbines," Doctor of Philiosophy, CREST, 2000.